

# COMPACT SCHEME FOR LASER-FREE THZ-SUB-THZ SOURCE\*

A. V. Smirnov<sup>#</sup>, RadiaBeam Technologies Inc., Santa Monica, CA 90404, USA

## Abstract

Undulator-free schemes based on resonant Cherenkov radiation in a small insertion device driven by a few MeV RF electron injector and alpha-magnet are considered. S- and C-band RF guns are compared to X-band multi-cell microlinac. Preference is given to planar radiator and wide quasi-flat sub-ps bunches that can be obtained with alpha magnet. It is shown that up to a milli-joule of sub-THz energy can be produced within a macropulse.

## INTRODUCTION

Relatively insignificant number of facilities such as synchrotron radiation sources and free electron lasers (FELs) around the world are dedicated specifically to the THz range to deliver substantial power to users. Obviously, more facilities are needed to cover the rapidly growing demand in dedicated sources for THz science and technology [1]. However, conventional radiation facilities based on FELs, electron storage rings, and/or energy recovery linacs (ERLs) are too large, expensive, and not readily available for a broader community of researchers, investigators, scientists and commercial applicants to operate it on a flexibly customized, on-demand, independent base. For narrow bandwidth radiation generation, resonant Cherenkov radiation is an attractive alternative to undulator radiation due to relative frequency independency from the beam energy (for relativistic beams) and due to the much higher equivalent shunt impedance. Coherence is provided by the Cherenkov synchronism between the microbunches and fundamental (or one of the lowest) eigenmode(s) along the interaction space hundreds of wavelengths long.

## THE CONCEPT

This source concept illustrated in Fig. 1 can be utilized for container inspection, screening, safe imaging, cancer diagnostics, surface defectoscopy, and many other applications. Substantial average power can be provided by using thermionic, plasma [2], field [3] or secondary emission [4] that can be perfectly combined with RF cavity.

The THz radiation is generated by beam pre-bunching and chirping in the RF gun, followed by microbunching in a magnetic compressor and resonant Cherenkov radiation of an essentially flat beam in a robust, planar, structure with mm-sub-mm gap. The proof-of-principle has been successfully demonstrated recently on a 5 MeV beam driven by an L-band thermionic injector [5].

We calculate the energy radiated by a single microbunch using the modal energy loss found analytically with the eigenmode excitation theory applied in time domain [6] for matched outcoupling without

trapped modes as follows:

$$W_{\text{tb}} \approx \frac{\omega rL}{4 Q} \frac{(q|\Phi|)^2}{|1 - \beta_{\text{gr}}/\beta|} \left( \frac{1 - \exp(-\alpha L)}{\alpha L} \right)^2, \quad (1)$$

where  $\omega = 2\pi f = h(\omega)v$  is the circular frequency of the resonant Cherenkov radiation,  $h(\omega)$  is the wavenumber defined by the structure dispersion,  $q$  is the bunch charge,  $r = E_z^2/dP/dz$  is the shunt impedance,  $\beta = v/c$ ,  $Q$  is the Q-factor,  $Q|\beta - \beta_{\text{gr}}| \gg 1$ ,  $\alpha = \pi f/Qv_{\text{gr}}$  is the attenuation, and  $\Phi = \exp(-(\omega\sigma_t)^2/2)$  is the formfactor for a Gaussian bunch having rms duration  $\sigma_t$ . Note Eq. (1) applied to, e.g., the 270 GHz setup [7], gives 9  $\mu\text{J}$  energy which is the same as measured [7].

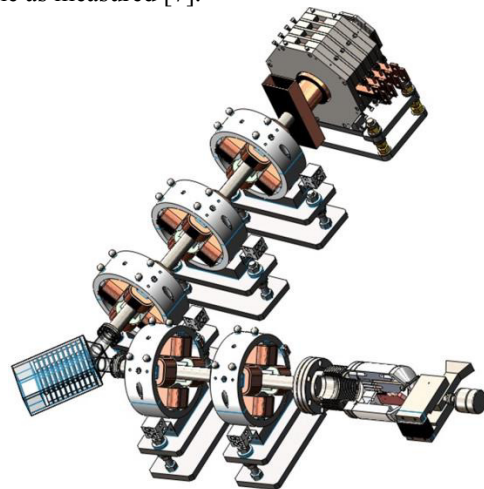


Figure 1: Schematics of the THz source beamline composed by quadrupoles, PM  $\alpha$ -magnet, Cherenkov radiator, dipole magnet, and THz beam output.

Below we consider only briefly key features of beam dynamics, slow-wave structure, and general beamline design.

## PLANAR CHERENKOV RADIATOR

Electromagnetic and mechanical engineering of a planar radiator [5,8,9] is used here as a prototype for a 0.67 THz radiator design shown in Fig. 2. The structure parameters are the following:  $r/Q=8 \text{ k}\Omega/\text{m}$  at 3 mm width of the grating, 0.6 mm interaction gap and 42  $\mu\text{m}$  groove height;  $Q=1410$ , and 1" structure length.

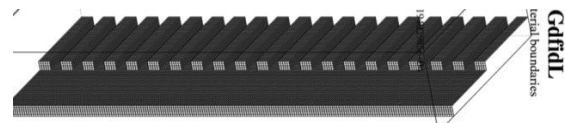


Figure 2: 20-period, bottom-half fragment of the planar radiator structure in GdfidL model (antenna horn is not shown).

\*Work supported by US DoE Contract DE- SC-FOA-0000760  
#asmirnov@radiabeam.com.

Results of time domain GdfidL code [10] and analytical [6] simulations are in a good accordance and given in Figs 3-5 for 50 pC charge, 200 fs rms duration (60  $\mu$ m rms length) bunch having  $\sim 0.7$  formfactor  $\Phi$ .

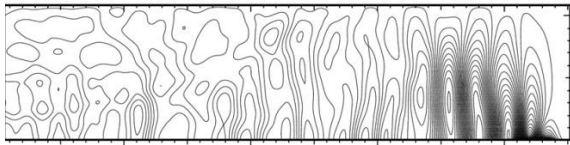


Figure 3: GdfidL contour plot in the median plane of the longitudinal electric field component of the wake induced in the 40-period SWS at  $t=15.2$  ps.

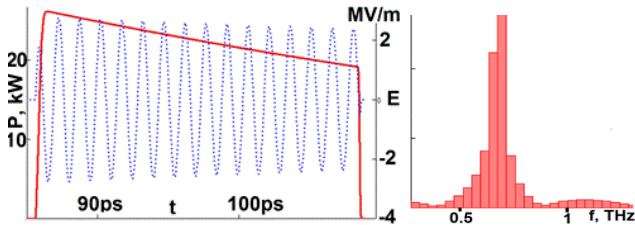


Figure 4: LEFT: Power (red) and field (blue) at the end of the structure vs. time. RIGHT: Field spectrum.

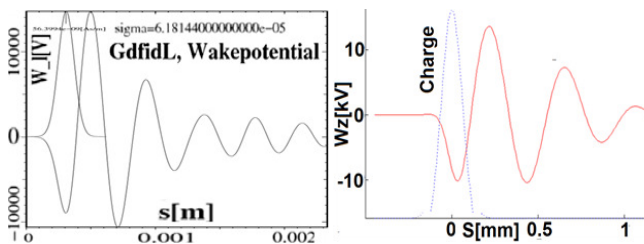


Figure 5: Wakepotential calculated numerically (left) and analytically (right) for 70 pC charge in the 40-period structure.

### BEAM DYNAMICS SIMULATIONS

Performance features of the rugged, high group velocity, planar radiator imply forming of sub-mm long, sub-mm tall, and mm-cm wide bunches to efficiently utilize the low-energy beam having substantial emittance (compared to photoinjector not used here). We simulated with ASTRA code [11] 1.6 cell thermionic RF guns producing 1.8 MeV energy-modulated beam in S- and C-bands using BNL/UCLA/SLAC cavity shape. Field profiles used for S- and C-band RF gun simulations are shown in Fig. 6 to produce 1.8 MeV, 90 pC bunch with  $\sim 11\mu$ m normalized emittance. Cathode radius is 1 mm, for S-band and 0.5 mm for C- band (with cathode loading  $\sim 17$  and 86 A/cm<sup>2</sup> respectively).

The beamline with the alpha-magnet have been optimized with ELEGANT for minimum vertical and longitudinal bunch dimensions in the radiator. The results are exemplified in Figs 7, 8 for C-band variant with 5 quadrupoles.

For X- band variant we considered here a biperiodic, 45-cell, tapered, side-coupled, 2 MeV microlinac designed and developed at RadiaBeam [12]. The microlinac structure was modified by using slightly longer regular

cells to provide energy chirp simulated with PARMELA code [13] (see Fig. 9).

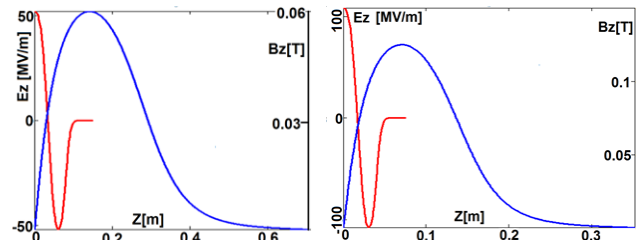


Figure 6: RF and magnetic field profiles used for 1.6-cell RF S-band (left) and C-band (right) gun ASTRA simulations.

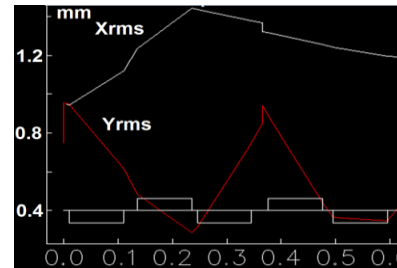


Figure 7: Transverse RMS dimensions for 1.8 MeV 90pC bunch along 5-quad beamline optimized with ELEGANT together with  $\alpha$ -magnet and energy filter (scraper) having 27% transmission.

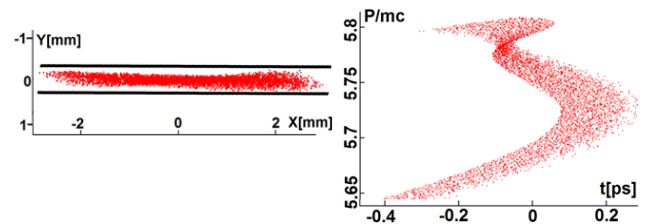


Figure 8: LEFT: Transverse beam profile in the 0.6mm interaction gap for C-band variant with 5 quadrupoles. RIGHT: Longitudinal phase space of the beam in the gap.

The beamline with 3 quadrupoles and  $\alpha$ -magnet was optimized with ELEGANT code [14]. Benefit of energy filtering related to formfactor (see Eqn. (1)) is shown in Fig. 10. The ELEGANT results are compared to the GPT code [15] simulations with taking into account space charge in the beamline (see Fig. 11).

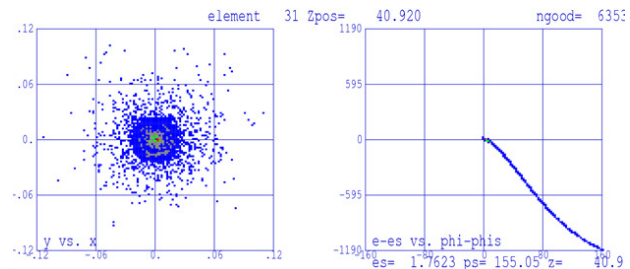


Figure 9: Transverse beam profile (left) and longitudinal phase space (right) for modified RadiaBeam biperiodic microlinac with side cells. Bunch charge 2 pC.

In Table 1 we summarized performance calculated for different beamlines with time domain model for 1" long

planar radiator having  $0.6 \times 10 \text{ mm}^2$  interaction gap, 3.7 M $\Omega$ /m shunt impedance,  $\beta_{gr}=0.8$  for 90 pC bunches produced from different RF injectors at 0.1% duty factor and 4  $\mu\text{s}$  pulse length.

In Table 2 we characterize a low power 0.67 THz source driven by 2 MeV 9.4 GHz microlinac using 1" long,  $0.6 \times 3.2 \text{ mm}^2$  interaction gap planar radiator having 11.3 M $\Omega$ /m shunt impedance,  $\beta_{gr}=0.8$  for 2 pC bunches having no losses in the radiator at 0.1% duty factor and 2.5  $\mu\text{s}$  pulse length.

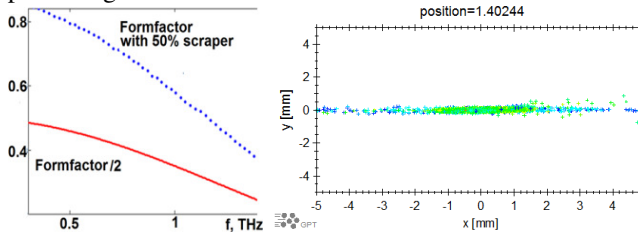


Figure 10: LEFT: Formfactor vs. frequency for the beam driven by RadiaBeam microlinac and microbunched in the beamline with and without energy filtering. RIGHT: Transverse beam profile simulated with GPT in the radiator having 0.6 mm vertical gap.

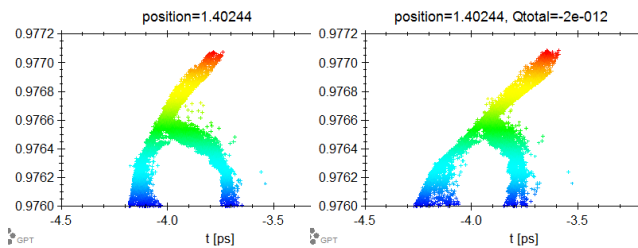


Figure 11: GPT simulations of longitudinal phase space without (left) space and including (right) charge in the beamline with 50% energy filtering.

Table 1: Simulated performance for the 0.67 THz source driven by S- and C- Band RF guns

Variant (RF band & # of quads)	Transmission			Bunches $\sigma$ , fs	Wmicro, nJ	Pmicro, kW	Wmacro, $\mu\text{J}$	Pmacro, W
	Charge, pC	Scraper, %	Radiator, %					
S-b 5q	13	15	94	105	46	2.2	524	131
S-b 3q	10	18	65	117	30	1.4	338	85
C-b 5q	25	28	100	130	165	7.8	3372	943
C-b 3q	17	27	68	105	78	3.7	1785	446

Table 2: Source performance with microlinac

Rep rate, Hz	Pulse t, $\mu\text{s}$	Charge, pC	$\sigma_c$ , fs	Micropulse Energy, nJ	Peak THz power, W	Average THz power, mW	Macropulse THz power, W
40	2.5	2	132	2.4	23	2.3	23

## CONCLUSION

Alpha magnet and quadrupoles can produce flat beams with a moderate aspect ratio  $\sim 10$  making a good match to the gap of planar radiator. C-band RF gun is very promising configuration for the system and capable to produce a kW power within a macropulse.

## ACKNOWLEDGMENT

The author is grateful to Bas van der Geer and Marieke de Loos for the GPT code simulations and Warner Bruns for the opportunity to use GdfidL code.

## REFERENCES

- [1] S. Chattopadhyay, S. T. Corneliussen, G. P. Williams, "Emerging Concepts, Technologies and Opportunities for Mezzo-Scale Terahertz and Infrared Facilities", THPKF084, EPAC'04, Lucerne, Switzerland p. 2454 (2004).
- [2] G. Xia, M. Harvey, A. J. Murray, W. Bertsche, R. Appleby, S. Chattopadhyay. IPAC2013, Shanghai, China (2013) 452.
- [3] V.N.Volkov et al., APAC'01, Beijing, China, p. 170 (2001).
- [4] N.Y. Huang, H. Hama, IPAC'10, Kyoto, Japan, p. 4683 (2011).
- [5] R. Agustsson, A. V. Smirnov et al. "Development of a Compact Insertion Device For Coherent Sub-Mm Generation", IPAC'13, WEPWA080, Shanghai, p. 2295 (2013).
- [6] A.V. Smirnov, Nucl. Instrum. Methods Phys. Res., Sect. A 480 (2-3) 387 (2002).
- [7] A.M. Cook et al. Phys. Rev. Lett. 103, 095003 (2009).
- [8] A.V. Smirnov, "A Ps-Pulsed E-Gun Advanced to a T-Wave Source of MW-Level Peak Power", RUPAC'12, Saint-Petersburg, September 2012, TUPPB052, p. 430 (2012).
- [9] A. Smirnov et al., "Performance of Planar Radiator in the RadiaBeam-IAC Experiment", WEPBA18, these proceedings.
- [10] W. Bruns, "The GdfidL Electromagnetic Field Simulator", <http://www.gdfidl.de>
- [11] K. Floettmann, "ASTRA A Space Charge Tracking Algorithm", Version. 3, DESY, Hamburg, Germany (2011).
- [12] S. Boucher, R. Agustsson, L. Faillace, J. Hartzell, A. Murokh, A. Smirnov, S. Storms, K. Woods. In Proceedings of IPAC2013, Shanghai, China, p. 3746 (2013).
- [13] L. M. Young, "Pamela", Documentation by J. H. Billen, Los Alamos National Laboratory, LA-UR-96-1835, December 2005.
- [14] M. Borland, "User's Manual for elegant", Program Version 25.0.2, Advanced Photon Source, March 2012.
- [15] B. Geer, M. Loos, "The General Particle Tracer code", Pulsar Physics, the Netherlands, April 2001.